An avenue of eddies: Quantifying the biophysical properties of mesoscale eddies in the Tasman Sea

J. D. Everett,[1,2,3] M. E. Baird,[2,3] P. R. Oke,[4] and I. M. Suthers[1,2]

Received 11 July 2012; accepted 14 July 2012; published 28 August 2012.

[1] The Tasman Sea is unique - characterised by a strong seasonal western boundary current that breaks down into a complicated field of mesoscale eddies almost immediately after separating from the coast. Through a 16-year analysis of Tasman Sea eddies, we identify a region along the south-east Australian coast which we name 'Eddy Avenue' where eddies have higher sea level anomalies, faster rotation and greater sea surface temperature and chlorophyll *a* anomalies. The density of cyclonic and anticyclonic eddies within Eddy Avenue is 23% and 16% higher respectively than the broader Tasman Sea. We find that Eddy Avenue cyclonic and anti-cyclonic eddies have more strongly differentiated biological properties than those of the broader Tasman Sea, as a result of larger anticyclonic eddies formed from Coral Sea water depressing chl. *a* concentrations, and for coastal cyclonic eddies due to the entrainment of nutrient-rich shelf waters. Cyclonic eddies within Eddy Avenue have almost double the chlorophyll *a* (0.35 mg m^{-3}) of anticyclonic eddies (0.18 mg m^{-3}). The average chlorophyll *a* concentration for cyclonic eddies is 16% higher in Eddy Avenue and 28% lower for anticyclonic eddies when compared to the Tasman Sea. With a strengthening East Australian Current, the propagation of these eddies will have significant implications for heat transport and the entrainment and connectivity of plankton and larval fish populations. **Citation:** Everett, J. D., M. E. Baird, P. R. Oke, and I. M. Suthers (2012), An avenue of eddies: Quantifying the biophysical properties of mesoscale eddies in the Tasman Sea, *Geophys. Res. Lett.*, *39*, L16608, doi:10.1029/2012GL053091.

1. Introduction

[2] The accumulation of more than a decade of satellite observations has provided the opportunity to examine the physical and biological interactions of mesoscale eddies at large temporal and spatial scales [*Kurian et al.*, 2011; *Isern-Fontanet et al.*, 2003; *Chelton et al.*, 2011a, 2011b]. Eddies are important contributors to the physical mechanisms of heat transport [*Jayne and Marotzke*, 2002] and movement of specific water masses [*Baird and Ridgway*, 2012]. Eddies stimulate and support primary (phytoplankton) [*McGillicuddy et al.*, 1998] and secondary (zooplankton) production [*Everett et al.*, 2011] and increase the abundance and survival of larval fish [*Logerwell and Smith*, 2001]. They also play a significant role in the transport of marine organisms to and from the coast and offshore regions [*Moore et al.*, 2007]. The boundaries of eddies and the surrounding water is also an important region of enhanced production [*Lima et al.*, 2002] and a foraging ground for marine and aerial predators [*Tew Kai et al.*, 2009].

[3] The western Tasman Sea is characterised by the presence of the poleward-flowing East Australian Current (EAC) and its associated mesoscale eddy field [*Nilsson and Cresswell*, 1981]. The EAC is the major western boundary current of the South Pacific sub-tropical gyre and originates in the warm oligotrophic waters of the Coral Sea and flows southward along the offshore edge of the continental shelf [*Hamon*, 1965]. Between 30°S and 34°S the EAC separates from the coast [*Godfrey et al.*, 1980], generating uplift of nutrient-rich slope water onto the continental shelf [*Oke and Middleton*, 2000]. South of the separation zone the EAC meanders eastward across the Tasman Sea, leaving behind a dynamic southward moving eddy field [*Ridgway and Godfrey*, 1997].

[4] Eddies in western boundary current systems, such as the Gulf Stream and Kuroshio, have previously been quantified at various degrees of spatial and temporal resolutions [*Brown et al.*, 1986; *Ebuchi and Hanawa*, 2000]. Tasman Sea eddies have been studied using satellite drifters [*Cresswell and Legeckis*, 1986], Geosat satellite altimetry [*Morrow et al.*, 1992, 1994], shipboard observations [*Cresswell*, 1982; *Everett et al.*, 2011], autonomous glider observations [*Baird et al.*, 2011; *Baird and Ridgway*, 2012] and numerical models [*Oke and Griffin*, 2011]. However no large-scale spatial and temporal analysis of the size, abundance and biophysical properties of Tasman Sea eddies has been undertaken to date. Significantly, the western Tasman Sea has the second fastest warming trend of all western boundary currents [*Wu et al.*, 2012], with cascading changes to ecological communities such as zooplankton populations and kelp beds already apparent [*Johnson et al.*, 2011]. In order to quantify the importance of processes such as heat transport, plankton productivity and larval fish survival and connectivity associated with eddies in the western Tasman Sea, knowledge of eddy characteristics in time and space is required.

[5] In this study we quantify the remotely-sensed sea surface temperature (SST) and chlorophyll *a* (chl. *a*) of eddies in the Tasman Sea, and then in an eddy-rich region in the western Tasman Sea we hereafter refer to as 'Eddy Avenue'.

[1]Evolution and Ecology Research Centre, University of New South Wales, Sydney, New South Wales, Australia.
[2]Sydney Institute of Marine Science, Mosman, New South Wales, Australia.
[3]Plant Functional Biology and Climate Change Cluster, University of Technology Sydney, Sydney, New South Wales, Australia.
[4]CSIRO Marine and Atmospheric Research, Hobart, Tasmania, Australia.

Corresponding author: J. D. Everett, Evolution and Ecology Research Centre, University of New South Wales, Sydney, NSW 2052, Australia. (jason.everett@unsw.edu.au)

0094-8276/12/2012GL053091

Table 1. Eddy Statistics as Derived From the *Chelton et al.* [2011b] Dataset[a]

	Cyclonic			Anticyclonic		
	Global	Tasman Sea	Eddy Avenue	Global	Tasman Sea	Eddy Avenue
Total abundance of Eddies	1081148	14094	1314	1057052	14892	1299
Daily abundance of Eddies (d^{-1})	1295	16.8	1.6	1266	17.8	1.6
Radii (km)	86	83	92	86	82	95
Sea Level Anomaly (cm)	7	10	23	6	10	24
Rotational Speed	16	23	45	15	23	50

[a]The table is split into cyclonic and anticyclonic eddies, and three regions: Global, Tasman Sea and Eddy Avenue. Apart from the total and daily 'abundance of eddies', all values displayed are averages for each of the three regions.

Eddies from within Eddy Avenue are shown to have different properties to the broader Tasman Sea, in part due to their direct interaction with the EAC and continental shelf.

2. Methods

2.1. Eddy Detection

[6] *Chelton et al.* [2011b] provides a publicly available global census of eddies determined from sixteen years of Sea Surface Height (SSH) fields derived from altimetry. Due to the filtering of the SSH fields, eddies of radii <40 km are generally not resolvable. For a full discussion of the methods used to identify and track eddies see *Chelton et al.* [2011b]. In this paper we analyse the dataset provided by *Chelton et al.* [2011b] for the region 26°S to 46°S and 148°E to 164°E in the Tasman Sea. Our analysis spans the period January 1993 to December 2008.

[7] Tracking eddies is the most difficult part of this process (compared to eddy-identification), especially within Western Boundary Current systems, because eddies split and merge during their lifetime resulting in imprecise calculations of the number, location and track of distinct eddies. In this paper, we deal specifically with 'eddy detections' rather than the number of unique eddies. The eddies in the online database are restricted to >4 week lifetimes so eddies that persist for less than this are not considered.

2.2. Remotely-Sensed Observations

[8] The SST and chl. *a* concentration of the eddies, and their climatological anomaly are calculated for all eddies where satellite data is available. SST is extracted from Legacy Bureau of Meteorology SST (LBoMSST), a 0.01° daily composite product derived from 1.1 km High Resolution Picture Transmission (HRPT) Advanced Very High Resolution Radiometer (AVHRR) subskin (~1 mm) SST. Chl. *a* is daily MODIS-Aqua 4 km (L3) data retrieved from OceanColor Web at Goddard Space Flight Center. Satellite data is used up to 2 days from the time of eddy observation. The mean value of an ~144 km^2 area in the eddy-centre was used to determine the eddy SST (12 × 12 pixels) and surface chl. *a* concentration (3 × 3 pixels). SST and chl. *a* anomalies were calculated using an AVHRR and MODIS-Aqua climatology at the same location for the corresponding day (AVHRR) or month (MODIS-Aqua) of the year.

2.3. Conceptual Model of Eddy Properties

[9] A simple conceptual model to describe eddy surface properties states that cyclonic eddies have a negative Sea Level Anomaly (SLA) and SST anomaly (SSTA) and lift nutrient rich waters towards the surface, resulting in a higher surface chl. *a* concentration (Figure S1c in the auxiliary material).[1] Anticyclonic eddies have a positive SLA and SSTA with a deeper surface mixed layer and therefore a lower surface chl. *a* concentration (Figure S1b). Beyond the model there is a significant spread in eddy properties (Figures S1a and S1d). The vertical processes driving these surface signatures are further discussed in the auxiliary material.

3. Results

3.1. Tasman Sea Eddies

[10] This study identified 14094 cyclonic and 14892 anticyclonic eddies within the Tasman Sea between January 1993 and December 2008 (Table 1). This is equivalent to a density of 61 cyclonic and 63 anticyclonic eddies per 10,000 km^2. On any given day there are 16.8 cyclonic and 17.8 anticyclonic eddies within the Tasman Sea. Tasman Sea eddies are typically smaller than the global average (~82 km radii compared with ~86 km), have a faster rotational speed (~23 cm s^{-1} compared with ~15–16 cm s^{-1}) and have a larger SLA (~10 cm compared with ~6–7 cm) (Table 1).

3.2. Eddy Avenue

[11] A region of high eddy activity is evident south of the point of separation of the EAC from the coast and is referred to as 'Eddy Avenue' (Figure 1). This region has historically been identified as a region of high eddy activity [*Morrow et al.*, 1992]. Eddy Avenue exhibits a high abundance of eddies between 32°S and 39°S, with the majority clustered north of 37°S. We identify 1314 cyclonic and 1299 anticyclonic eddies within Eddy Avenue (Table 1), at a density of 75 cyclonic and 74 anticyclonic eddies per 10,000 km^2.

[12] Eddy Avenue also contains the most energetic eddies in terms of SLA, rotational speeds and radii when compared to both the Tasman Sea and the global census (Figure 1 and Table 1). The global and Tasman Sea eddies have similarly skewed distributions towards the lower end of the scale for amplitude, radius and rotational speed (Figure 2). The eddies within Eddy Avenue have a quasi-normal distribution, with peaks in the distribution of amplitude and rotational speed at higher values compared to the Tasman Sea as a whole. Eddies in Eddy Avenue often have a SLA >15 cm and a rotational speed >30 cm s^{-1} (Figure 2). The long tails in the distribution of amplitude and rotational speeds in the Tasman Sea are due to Eddy Avenue eddies. Similarly, the

[1]Auxiliary materials are available in the HTML. doi:10.1029/2012GL053091.

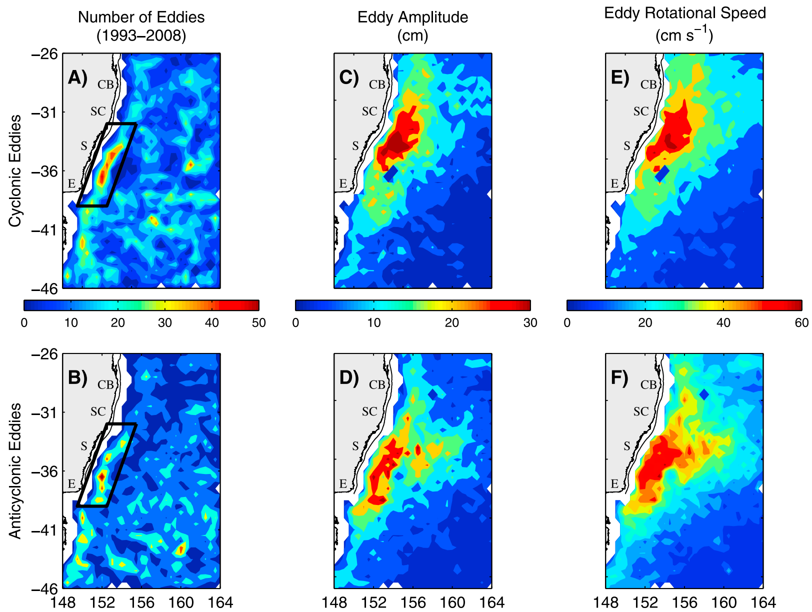

Figure 1. Eddy contour map showing (a, b) the total number of eddies, (c, d) mean amplitude, and (e, f) mean rotational speed for cyclonic and anticyclonic eddies, respectively. The centre-point of each eddy, as defined by *Chelton et al.* [2011b] were binned into 0.5° × 0.5° grid boxes. CB = Cape Byron, SC = Smoky Cape, S = Sydney, E = Eden. Note: This analysis shows weekly eddy detections. An eddy which had a lifetime of 4 weeks, will appear on this plot 4 times. The area identified as 'Eddy Avenue' is denoted by a black box in Figures 1a and 1b.

long tail in global eddies is primarily due to the energetic boundary current eddies in the Kuroshio, Agulhas, Gulf Stream, Brazil Current and the EAC [see *Chelton et al.*, 2011b, Figure 10].

3.3. Anomalies of Sea-Surface Temperature and Surface Chlorophyll *a*

[13] SSTA for 4663 cyclonic and 4850 anticyclonic Tasman Sea eddies and SCA for 3768 cyclonic and 3571 anticyclonic Tasman Sea eddies are analysed. Tasman Sea cyclonic eddies have a negative SSTA in 56% of cases (Figure 3a), with a mean SSTA of −0.11°C (Table 2). Tasman Sea anticyclonic eddies have a positive SSTA in 78% of cases (Figure 3e) with a mean SSTA of +0.59°C (Table 2). Cyclonic Tasman Sea eddies have a positive chl. *a* anomaly in 49% of cases (Figure 3b) with a mean SCA of only +0.016 mg m^{-3}. Anticyclonic eddies have a negative SCA 72% of cases (Figure 3f) with a mean anomaly of −0.042 mg m^{-3}. The SST and chl. *a* signal of cyclonic eddies is not as clear as it is for the anticyclonic eddies as the background temperature of the Tasman Sea is relatively cold.

[14] Within Eddy Avenue, surface SST anomalies for 456 cyclonic and 457 anticyclonic eddies were identified, along with chl. *a* anomalies for 401 cyclonic and 364 anticyclonic eddies. Within Eddy Avenue, 71% of cyclonic eddies have a negative SSTA (Figure 3c) with a mean SSTA of −0.62°C (Table 2), while anticyclonic eddies have a positive anomaly in 67% of cases (Figure 3g) with a mean SSTA of +0.32°C (Table 2). Cyclonic eddies in Eddy Avenue show a positive SCA in 65% of cases (Figure 3d) with a mean anomaly of

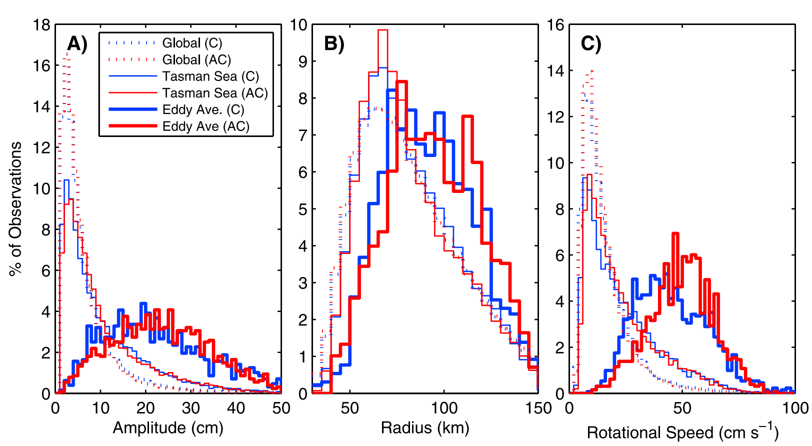

Figure 2. A histogram of the (a) amplitude (cm), (b) radius (km) and (c) rotational speed (cm s^{-1}) of cyclonic (blue) and anticyclonic (red) eddies. The global ocean, Tasman Sea and Eddy Avenue are shown separately. The data is binned into 1 cm (amplitude), 5 km (radius) and 2 cm s^{-1} (rotational speed) bins.

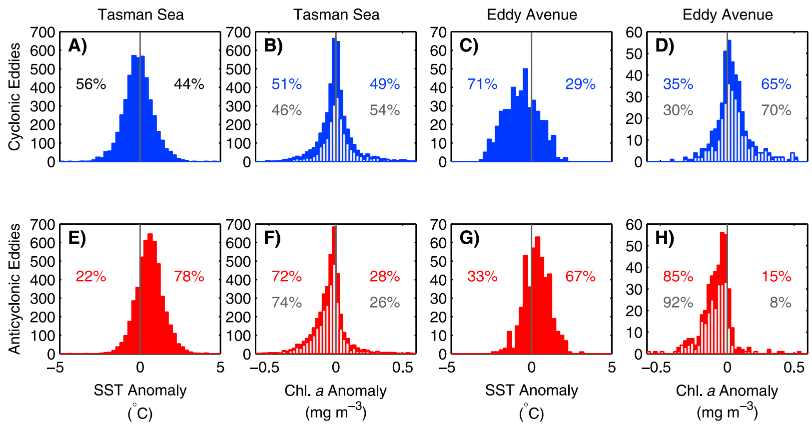

Figure 3. A histogram of the SST and chl. *a* climatological anomaly for the Tasman Sea and Eddy Avenue. Cyclonic eddies (a–d) and anticyclonic eddies (e–h) are shown separately. The percentage of observations each side of zero anomaly are shown in each panel. SCA are shown for all eddies (blue/red), and for a subset excluding warm-surface cyclonic eddies and cool-surface anticyclonic eddies (grey), with the percentages also in grey.

+0.070 mg m^{-3} (Table 2), while anticyclonic eddies have a negative SCA in 85% of cases (Figure 3h) with a mean SCA of −0.083 mg m^{-3} (Table 2). The Eddy Avenue cyclonic eddies have a more negative SSTA and greater SCA than those for the broader Tasman Sea, while anticyclonic eddies have a greater negative SCA than the broader Tasman Sea. The anticyclonic SSTA is less in Eddy Avenue than the broader Tasman Sea, in part due to Eddy Avenue commonly containing large anticyclonic eddies.

3.4. Deviations From the Conceptual Model of Eddy Surface Properties

[15] Given our conceptual model of eddies (Section 2.3) it is expected that a cyclonic eddy will have a negative SSTA and an anticyclonic eddy a positive SSTA. A large fraction of the cyclonic (44%) and anticyclonic eddies (22%) in the Tasman Sea did not conform to this model. If the above analysis of SCA is repeated, excluding those eddies which do not conform to the SSTA model, the relationship between SST and chl. *a* becomes stronger (Figures 3b, 3d, 3f, and 3h and Table 2). In particular, anticyclonic eddies in Eddy Avenue have a negative SCA in 92% of cases (Figure 3h, grey bars) with a mean of −0.101 mg m^{-3} (Table 2). Similarly, Eddy Avenue cyclonic eddies have a positive SCA in 70% of cases (Figure 3d, grey bars), with a mean of +0.097 mg m^{-3} (Table 2). It is likely that the eddies which did not conform to the conceptual model did so due to two reasons. Firstly, because of errors in estimating the centre of non-circular eddies in the census, or secondly due to surface anomalies such as surface flooding or mixing, not reflecting the underlying eddy properties (see auxiliary material).

4. Discussion and Conclusions

[16] Eddy Avenue is identified as a region of the western Tasman Sea where eddies have higher SLA's, faster rotation and greater SSTA's and SCA's. The density of cyclonic and anticyclonic eddies within Eddy Avenue is 23% and 16% higher respectively than the broader Tasman Sea. Globally, eddy formation generally occurs at the eastern boundaries of the ocean basins, before the eddies propagate westward and terminate near the western boundaries [*Chelton et al.*, 2011b]. In the western Tasman Sea however we typically observe that eddies are generated through instabilities associated with the EAC flow [*Bowen et al.*, 2005].

[17] The location of eddy formation and their subsequent propagation affects eddy properties, in particular chl. *a* concentration. The average chl. *a* concentration for all cyclonic eddies is 16% higher in Eddy Avenue than the Tasman Sea and the SCA is four-times higher in Eddy Avenue (Table 2). This elevated chl. *a* is likely to be a result of the cyclonic eddies propagating close to the continental shelf and entraining coastal waters, enriched in plankton and larval fish. Coastal cyclonic eddies are reported to hold the key to the survival and recruitment of fish larvae in the Kuroshio system [*Kasai et al.*, 2002], and are thought to play a similar role in Eddy Avenue [*Suthers et al.*, 2011]. The success of this mechanism depends upon the regular encroachment of cyclonic eddies onto the shelf. Within

Table 2. Remotely-Sensed SST and Chl. *a* Concentration for Eddies Identified in the *Chelton et al.* [2011b] Dataset[a]

	Cyclonic		Anticyclonic	
	Tasman Sea	Eddy Avenue	Tasman Sea	Eddy Avenue
Number of SST obs.	4663	456	4850	457
Mean SST (°C)	17.60	19.41	18.02	20.41
Mean SSTA (°C)	−0.11	−0.62	+0.59	+0.32
Number of chl. *a* obs.	3768 (2160)	401 (287)	3571 (2780)	364 (238)
Mean chl. *a* (mg m^{-3})	0.30 (0.31)	0.35 (0.38)	0.25 (0.24)	0.18 (0.17)
Mean SCA (mg m^{-3})	+0.016 (+0.028)	+0.070 (+0.097)	−0.042 (−0.047)	−0.083 (−0.101)

[a]The number of observations (obs.) used for SST/Chl *a* analysis are listed in the row prior to the SST and chl. *a* values respectively. The table is split into cyclonic and anticyclonic eddies. Bracketed values in the chl. *a* rows are those for which the SSTA agreed with the SLA.

Eddy Avenue there are ~1.5 cyclonic eddies on any given day (Table 1) indicating this is likely a regular occurrence.

[18] Conversely, anticyclonic eddies within Eddy Avenue have on average 28% less chl. *a*, and a SCA that is twice as negative, when compared to the Tasman Sea (Table 2). This is primarily due to anticyclonic eddies being generated from the southward flowing waters of the oligotrophic EAC. They retain a relatively low surface chl. *a* concentration by not mixing horizontally with the surrounding water. They have been shown to maintain their zooplankton community of origin over many months after propagating into the cooler Tasman Sea waters [*Griffiths and Brandt*, 1983].

[19] Within the region of Eddy Avenue, submesoscale cyclonic eddies are common and have been shown to have increased chl. *a* concentrations and abundance of zooplankton at their centre [*Everett et al.*, 2011]. Further, submesoscale eddies can obscure the larger mesoscale patterns by introducing heterogeneity within and between the larger mesoscale eddies. Nonetheless, it is clear that the scale that dominates the interactions between physical and biological processes in Eddy Avenue, and to a lesser extent the Tasman Sea, is the mesoscale.

[20] **Acknowledgments.** This research was funded by ARC Discovery Project DP0881182 held by IMS and PO. JDE is partly supported by funding from the NSW SLF. The authors gratefully appreciate the global eddy census data provided by Dudley Chelton and Michael Schlax. We thank David Griffin (CSIRO) for useful discussions and Ken Ridgway (CSIRO) for providing the AVHRR climatology. The LBoMSST data was sourced from the Integrated Marine Observing System (IMOS), an initiative of the Australian Government being conducted as part of the National Collaborative Research Infrastructure Strategy and the Super Science Initiative. We also acknowledge the MODIS mission scientists and associated NASA personnel for the production of the data used in this research effort. The paper was greatly improved by the comments from two anonymous reviewers. This is publication 0075 of the Sydney Institute of Marine Science.

[21] The Editor thanks Peter Gaube and an anonymous reviewer for assisting in the evaluation of this paper.

References

Baird, M. E., and K. R. Ridgway (2012), The southward transport of sub-mesoscale lenses of Bass Strait Water in the centre of anti-cyclonic mesoscale eddies, *Geophys. Res. Lett.*, *39*, L02603, doi:10.1029/2011GL050643.

Baird, M. E., I. M. Suthers, D. A. Griffin, B. Hollings, C. B. Pattiaratchi, J. D. Everett, M. Roughan, K. Oubelkheir, and M. Doblin (2011), The effect of surface flooding on the physical-biogeochemical dynamics of a warm-core eddy off southeast Australia, *Deep Sea Res., Part II*, *58*(5), 592–605, doi:10.1016/j.dsr2.2010.10.002.

Bowen, M. M., J. L. Wilkin, and W. J. Emery (2005), Variability and forcing of the East Australian Current, *J. Geophys. Res.*, *110*, C03019, doi:10.1029/2004JC002533.

Brown, O., P. Cornillon, S. Emmerson, and H. Carle (1986), Gulf Stream warm rings: A statistical study of their behavior, *Deep Sea Res., Part A*, *33*, 1459–1473.

Chelton, D. B., P. Gaube, M. G. Schlax, J. J. Early, and R. M. Samelson (2011a), The influence of nonlinear mesoscale eddies on near-surface oceanic chlorophyll, *Science*, *334*, 328–332, doi:10.1126/science.1208897.

Chelton, D. B., M. G. Schlax, and R. M. Samelson (2011b), Global observations of nonlinear mesoscale eddies, *Prog. Oceanogr.*, *91*(2), 167–216, doi:10.1016/j.pocean.2011.01.002.

Cresswell, G. (1982), The coalescence of two East Australian Current warm-core eddies, *Science*, *215*(4529), 161–164.

Cresswell, G., and R. Legeckis (1986), Eddies off southeastern Australia, *Deep Sea Res., Part A*, *33*(11–12), 1527–1562, doi:10.1016/0198-0149(86)90066-X.

Ebuchi, N., and K. Hanawa (2000), Mesoscale eddies observed by TOLEX-ADCP and TOPEX/POSEIDON altimeter in the Kuroshio recirculation region south of Japan, *J. Oceanogr.*, *56*, 43–57.

Everett, J. D., M. E. Baird, and I. M. Suthers (2011), Three-dimensional structure of a swarm of the salp *Thalia democratica* within a cold-core eddy off southeast Australia, *J. Geophys. Res.*, *116*, C12046, doi:10.1029/2011JC007310.

Godfrey, J., G. Cresswell, T. Golding, A. Pearce, and R. Boyd (1980), The separation of the East Australian Current, *J. Phys. Oceanogr.*, *10*, 430–440.

Griffiths, F., and S. B. Brandt (1983), Mesopelagic Crustacea in and around a warm-core eddy in the Tasman Sea off eastern Australia, *Aust. J. Mar. Freshwater Res.*, *34*, 609–623.

Hamon, B. (1965), The East Australian Current, 1960–1964, *Deep Sea Res. Oceanogr. Abstr.*, *12*, 899–921.

Isern-Fontanet, J., E. García-Ladona, and J. Font (2003), Identification of marine eddies from altimetric maps, *J. Atmos. Oceanic Technol.*, *20*(5), 772–778.

Jayne, S., and J. Marotzke (2002), The oceanic eddy heat transport, *J. Phys. Oceanogr.*, *32*(12), 3328–3345.

Johnson, C. R., et al. (2011), Climate change cascades: Shifts in oceanography, species' ranges and subtidal marine community dynamics in eastern Tasmania, *J. Exp. Mar. Biol. Ecol.*, *400*(1–2), 17–32, doi:10.1016/j.jembe.2011.02.032.

Kasai, A., S. Kimura, H. Nakata, and Y. Okazaki (2002), Entrainment of coastal water into a frontal eddy of the Kuroshio and its biological significance, *J. Mar. Syst.*, *37*(1–3), 185–198, doi:10.1016/S0924-7963(02)00201-4.

Kurian, J., F. Colas, X. Capet, J. C. McWilliams, and D. B. Chelton (2011), Eddy properties in the California Current System, *J. Geophys. Res.*, *116*, C08027, doi:10.1029/2010JC006895.

Lima, I. D., D. B. Olson, and S. C. Doney (2002), Biological response to frontal dynamics and mesoscale variability in oligotrophic environments: Biological production and community structure, *J. Geophys. Res.*, *107*(C8), 3111, doi:10.1029/2000JC000393.

Logerwell, E., and P. Smith (2001), Mesoscale eddies and survival of late stage Pacific sardine (*Sardinops sagax*) larvae, *Fish. Oceanogr.*, *10*(1), 13–25.

McGillicuddy, D. J., A. Robinson, D. A. Siegel, H. Jannasch, R. Johnson, T. Dickey, J. McNeil, A. Michaels, and A. Knap (1998), Influence of mesoscale eddies on new production in the Sargasso Sea, *Nature*, *394*(6690), 263–266.

Moore, T. S., R. J. Matear, J. Marra, and L. Clementson (2007), Phytoplankton variability off the Western Australian coast: Mesoscale eddies and their role in cross-shelf exchange, *Deep Sea Res., Part II*, *54*(8–10), 943–960, doi:10.1016/j.dsr2.2007.02.006.

Morrow, R. A., J. A. Church, R. C. Coleman, D. B. Chelton, and N. White (1992), Eddy momentum flux and its contribution to the Southern Ocean momentum balance, *Nature*, *357*, 482–484.

Morrow, R. A., R. Coleman, and J. A. Church (1994), Surface eddy momentum flux and velocity variances in the Southern Ocean from Geosat altimetry, *J. Phys. Oceanogr.*, *24*, 2050–2071.

Nilsson, C., and G. Cresswell (1981), The formation and evolution of East Australian Current warm-core eddies, *Prog. Oceanogr.*, *9*(3), 133–183.

Oke, P. R., and D. A. Griffin (2011), The cold-core eddy and strong upwelling off the coast of New South Wales in early 2007, *Deep Sea Res., Part II*, *58*(5), 574–591, doi:10.1016/j.dsr2.2010.06.006.

Oke, P. R., and J. H. Middleton (2000), Topographically induced upwelling off eastern Australia, *J. Phys. Oceanogr.*, *30*(3), 512–531.

Ridgway, K. R., and J. S. Godfrey (1997), Seasonal cycle of the East Australian Current, *J. Geophys. Res.*, *102*(C10), 22,921–22,936.

Suthers, I. M., et al. (2011), The strengthening East Australian Current, its eddies and biological effects—An introduction and overview, *Deep Sea Res., Part II*, *58*(5), 538–546, doi:10.1016/j.dsr2.2010.09.029.

Tew Kai, E., V. Rossi, J. Sudre, H. Weimerskirch, C. Lopez, E. Hernandez-Garcia, F. Marsac, and V. Garçon (2009), Top marine predators track Lagrangian coherent structures, *Proc. Natl. Acad. Sci. U. S. A.*, *106*(20), 8245–8250, doi:10.1073/pnas.0811034106.

Wu, L., et al. (2012), Enhanced warming over the global subtropical western boundary urrents, *Nat. Clim. Change*, *2*(1), 1–6, doi:10.1038/nclimate1353.